Journal Pre-proof

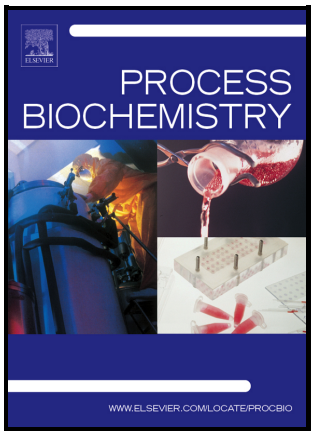

Characterization of the enzymes involved in the diol synthase metabolic pathway in *Pseudomonas aeruginosa*Running title: Diol-Synthase pathway enzymes

Shirin Shoja-Chaghervand, Mónica Estupiñán, Marc Castells, Francesc Rabanal, Yolanda Cajal, Angeles Manresa, Montserrat Busquets

PII: S1359-5113(22)00221-5

DOI: https://doi.org/10.1016/j.procbio.2022.06.017

Reference: PRBI12713

To appear in: *Process Biochemistry*

Received date: 10 January 2022
Revised date: 14 June 2022
Accepted date: 17 June 2022

Please cite this article as: Shirin Shoja-Chaghervand, Mónica Estupiñán, Marc Castells, Francesc Rabanal, Yolanda Cajal, Angeles Manresa and Montserrat Busquets, Characterization of the enzymes involved in the diol synthase metabolic pathway in *Pseudomonas aeruginosa*Running title: Diol-Synthase pathway enzymes, *Process Biochemistry,* (2022) doi:https://doi.org/10.1016/j.procbio.2022.06.017

Characterization of the enzymes involved in the diol synthase metabolic pathway in *Pseudomonas aeruginosa*

Running title: Diol-Synthase pathway enzymes

Shirin Shoja-Chaghervand[1], Mónica Estupiñán[1], Marc Castells[1], Francesc Rabanal[2], Yolanda Cajal[3], Angeles Manresa[1], Montserrat Busquets[4*]

[1]Department of Biology, Healthcare and the Environment. Faculty of Pharmacy and Food Sciences, University of Barcelona. Av. Joan XXIII 27-30, 08028 Barcelona, Spain.

[2]Department of Inorganic and Organic Chemistry. Organic Chemistry section. Faculty of Chemistry. University of Barcelona. Martí Franqués 1. 08028 Barcelona. Spain.

[3]Department of Pharmacy, Pharmaceutical Technology and Physical-chemistry. Faculty of Pharmacy and Food Sciences, University of Barcelona. Av. Joan XXIII 27-30, 08028 Barcelona, Spain

[4]Department of Biochemistry and Molecular Biomedicine. Faculty of Biology, University of Barcelona. Av. Diagonal 643, 08028 Barcelona, Spain.

*Author for correspondence: Montserrat Busquets e-mail: mbusquets@ub.edu

Abstract

This study is the first attempt to report the biochemical characterisation of the 10*S*-dioxygenase (10*S*-DOX) and 7*S*, 10*S*-diol synthase (7,10-DS). Both enzymes showed similar pH profiles with 10*S*-DOX presenting the highest activity at 30 ºC whereas 7,10-DS did not show a clear preferred temperature. These differences were reflected in the thermostability assay, the Km values were 0.89 ± 0.22 mM and 3.26 ± 0.31 mM for 10*S*-DOX and 7,10-DS, respectively. Inductively coupled plasma mass spectrometry indicated that both enzymes contained bound to heme group Fe^{2+} as a prosthetic group: 10*S*-DOX (0.95 mol Fe^{2+}/mol of protein) and 7,10-DS (1.18 mol Fe^{2+}/mol of protein), respectively. Assays using metal cations as cofactors revealed that Mg^{2+} and Ni^{2+} enhance 7,10-DS activity, whereas Hg^{2+} decrease it up to 50%. The activity of 10*S*-DOX in the presence of Mn^{2+} and Fe^{2+} was reduced to 51.6% and 61.8. Aggregated proteins producing 10*S*-DOX and 7,10-DS were characterised as inclusion bodies: IBs-77 and IBs-78 respectively, was performed by Fourier Transform spectroscopy (FT-IR), Atomic Force Microscopy, dye binding, and proteolysis.

The specific activity was 1.55 IU/mg for IBs-77 and 1.05 IU/mg for IBs-78. The presence of the oleate-diol synthase pathway in proteobacteria other than *Pseudomonas aeruginosa* was detected.

Keywords:

Oxylipins; diol synthase pathway; enzyme characterization; Inclusion bodies; proteobacteria

Abbreviations

10-H(P)OME:(10*S*)-hydro(pero-)xy-8(*E*)-octadecenoic acid; 10-HOME:(10*S*)-hydroxy-(8*E*)-octadecenoic acid; 10*S*-DOX: (10*S*)-dioxygenase; 7,10-DiHOME:(7*S*, 10*S*)-dihydroxy-(8*E*)-octadecenoic acid; 7,10-DS: Diol synthase; AFM: Atomic force microscopy; BSA: Bovine serum albumin; CatIBs: Catalytically-active inclusion body; CCP: Cytochrome c peroxidases; CR: Congo red; DMSO: dimethyl sulfoxide; ESI: Electrospray ionization; FadCCPs: Fatty acid-di-heme Cytochrome c peroxidases; FTIR: Fourrier Transform Infrared spectroscopy; HPLC: High performance liquid chromatography; IBs: Inclusion bodies; IBs-77: Inclusion bodies of 10*S*-DOX produced in *E. coli* DH5α / pMMB-10*S*-DOX; IBs-78: Inclusion bodies of 7,10-DS produced in *E. coli* BL21-7,10-DS; ICP-MS: Inductively coupled plasma mass spectrometer; IU: International unit; IPTG: Isopropil-β-D-1-tiogalactopiranósido;—LC- MS/MS: Liquid chromatography- Mass spectrometry; MS: Mass spectrometry; OA: Oleic acid; PBS: sodium phosphate buffer; PK: Proteinase K; RP-LC-MS/MS: Reverse phase-liquid chromatography-Mass spectrometry; SDS-PAGE: Sodium Dodecyl Sulfate Polyacrylamide Gel Electrophoresis;

1. Introduction

The biological relevance of oxylipins or oxygenate fatty acids as chemical mediators involved in the control of a large number of physiological processes has been reported in mammals, plants, fungi and bacteria. This is reflected in their participation in a wide range of key roles during inflammation, internal signalling, development and reproduction, motility, biofilm formation and virulence [1–4]. The functionalisation of the aliphatic hydrocarbon chain by reactive hydroxyl groups enables the synthesis of new compounds, acting as building blocks for new polymers generation as stabilisers and emulsifiers, and useful as starting materials for fine chemistry [5–7]. Oxylipins have been applied widely in cosmetic, chemical and food industries due to their physico-chemical properties as amphipathic molecules, constituting value-added compounds, which can be produced by renewable sources as oily wastes [8–10].

Fatty acid oxygenases are a diverse enzymatic group, which can be generally classified into two major classes of enzymes: heme-containing mono- and di-oxygenases and non-heme containing enzymes such as lipoxygenases. Fatty acid oxygenases are demonstrated to be widely distributed in eukaryotic organisms and several biocatalysts such as cytochrome P450 monooxygenases, prostaglandin H synthases, α-dioxygenases (alpha-DOX), linoleate diol synthases and lipoxygenases. They have been biochemically characterised by variations in their catalytic nature, and some cases, requiring the presence of cofactors [11]. In recent years, the extensive search for fatty acid oxygenases in prokaryotic organisms has facilitated the discovery, characterisation and crystallisation of the first bacterial lipoxygenases [12], as well as the identification of fatty acid-di-heme cytochrome C peroxidases (FadCCPs) [13]. To date, FadCCPs have been classified in a new subfamily of enzymes with two members, which can act as mono- and di-hydroxylating enzymes without cofactor supply and are attractive for green-technology applications [14]. These enzymes were identified in *P. aeruginosa* strains and are encoded by *PA2077* and *PA2078* genes, which constitute a fine-regulated operon belonging to the same metabolic pathway, known as the oleate-diol synthase route.

Oleate-diol synthase pathway unexpectedly differs from other previously characterised diol synthases as it consists of two sequentially and independently enzymatic reactions (Figure 1): first, oleic acid (OA) (as the preferred substrate), is initially converted into hydroperoxide 10-H(P)OME ((10*S*)-hydroxy(per)oxy-(8*E*)-octadecenoic acid) by a 10*S*-DOX (*PA2077*), followed by the bioconversion of the hydroperoxide into 7,10-DiHOME ((7*S*, 10*S*)-dihydroxy-(8*E*)-octadecenoic acid) by a 7*S*,10*S*-diol synthase (7,10-DS) (*PA2078*) [15]. Oleate-derived oxylipins 10-H(P)OME which is spontaneously reduced to 10-HOME ((10*S*)-hydroxy-(8*E*)-octadecenoic acid) and 7,10-DiHOME are synthesised in the periplasm of the cell and are specifically exported through ExFadLO outer-membrane transport to the extracellular medium, where they accumulate and act as a bioactive compound. The ExFadLO was reported as the first outer membrane transporter for exporting oxylipins in *P. aeruginosa* [16]. The FadCCPs enzymes might have originated from a genetic duplication event and functional evolution through mutagenesis, thereby acquiring different catalytic behaviours [14]. This is based on their high similarity, including the catalytic core of 10*S*-DOX and 7,10-DS which are composed of two confronted heme-binding groups described as cytochrome C peroxidases (CCPs) and their phylogenetic analysis as an extremely conserved transcriptional unit. Here, a complete description of FadCCPs subfamily 10*S*-DOX and 7,10-DS was performed through a whole biochemical characterisation of 10*S*-DOX and 7,10-DS as an initial step to deepen into their potential uses in green-technology applications and their importance in the impact of host-pathogen interactions in insect and plants cells.

Inclusion bodies (IBs) are aggregated unfolded proteins resulting from high-level expression [17]. In *Escherichia coli* recombinant bacterial cells, a commonly used heterologous host, IBs are enhanced by the use of high copy number plasmids, strong promoter systems or increasing inducer concentration/temperature [18,19]. IBs were initially identified as undesirable products, due to their catalytic activity (they contain about 50% of correctly folded protein), easy isolation and proteolytic resistance. Nevertheless, IBs have become useful particles in a wide range of applications such as immobilised biocatalysts for synthesis in biotechnology applications due to their high porosity, or as nanopills when delivering active substances within the cells, and nowadays are receiving great attention [19–21].

We report for the first time the biochemical characterization of the 10*S*-DOX and the 7*S*, 10*S*-diol synthase. The bioconversion of oleic acid into 10-H(P)OME, the substrate of the 10*S*-DOX, by a new recombinant *Pseudomonas putida* KT2440/pBBR-77. Moreover, the structure and morphology and functional activity of the IBs detected in *E. coli* DH5α/pMMB-77 and BL21/pET28a-78 were determined by FT-IR spectroscopy Th-T dye binding, proteolytic degradation assays and atomic force microscopy (AFM). Finally, the experimental screening for 10*S*-DOX and 7,10-DS activities in other proteobacteria was also determined.

2. Materials and methods

2.1 Materials

Fatty acids stock solutions (20 mM) were prepared in absolute ethanol (Panreac) or dimethyl sulfoxide (DMSO) (Sigma-Aldrich) and stored at -20 ºC. A homemade standard containing OA; 10-H(P)OME; 10-HOME and 7,10-DiHOME, [22] was used for the biochemical characterisation of the enzymes. Other fatty acids employed to determine substrate specificity are listed in Table S1 Solvents for organic extractions, chromatography mobile phase, LC and LC/MS were obtained from Panreac, Applichem, Carlo Erba Reagents and Fisher Scientific. All the chemicals were of American Chemical Society (ACS) grade quality.

2.2 Bacterial strains, media and growth conditions

Bacterial strains and plasmids used in this work are listed in Table I. All recombinant strains were grown overnight in TSB (17 g of casein peptone, 3 g soymeal peptone, 2.5 g glucose, 5 g

NaCl, and 2.5 g KH_2PO_4) at 30 ºC, on a rotary shaker operated at 150 rpm under aerobic conditions. Media were supplemented with antibiotics at the following concentrations: chloramphenicol 20 µg/ml for *E. coli* DH5α and chloramphenicol 400 µg/ml for *P. putida* KT2440. *P. putida* KT2440 was cloned with *PA2077*, inserted into pBBR plasmid and was used to produce 10-H(P)OME, the substrate for diol synthase enzyme [23].

2.3 Cloning and expression of 10*S*-DOX for in vitro production of 10-H(P)OME

Gene *PA2077* was amplified from *P. aeruginosa* PAO1 DNA genomic using specific primers (B77-R AGGATCCGACACCCAGTTCG, *BamH*I; K77-F AGGTACCCCACATGCCCAA, *Kpn*I). The amplified gene was cloned into *P. putida* pBBR-77 and *PA2077* and expressed in the shuttle plasmid pBBRMCS1. Cultures of *P. putida* KT2440/pBBR-77 were grown on TSB overnight at 30 ºC at 150 rpm; cells were harvested by centrifugation 10000 x g for 20 min and 3-fold concentrated in buffer Tris-HCl 50 mM pH 7.0. The cell suspension was adjusted at optical density, $O.D._{600nm}$ = 2.0, further sonicated (70% vibration amplitude and 3 cycles of 1 min; 0.5 s pulse rate) (Bandelin Sonopuls HD) and then centrifuged at 10000 x g in a Beckman benchtop centrifuge for 15 min. Next, 0.5 g/L of OA (90%) was added to the cell extract and incubated for 1 h at 30 ºC in a rotary shaker at 150 rpm. Products were extracted and detected by TLC and/or LC chromatography for monitoring 10-H(P)OME production.

DNA and amino acid sequences were obtained from The *Pseudomonas* Genome Database (www.pseudomonas.com). Blast searches were performed for nucleotide and amino acid sequence analysis to retrieve identity and similarity percentages by pairwise alignment. NCBI (http://www.ncbi.nlm.nih.gov) was used for multiple sequence alignment (MSA) [29].

2.4 Expression and purification of 10*S*-DOX and 7,10-DS

Genes *PA2077* and *PA2078* were individually amplified from *P. aeruginosa* PAO1 genomic DNA using specific primers for the *PA2077* gene (B77-R AGGATCCGACACCCAGTTCG, *BamHI*; B77-F AGGTACCCCACATGCCCAA, *Kpn*I; and *PA2078* gene (B78-R AGGATCCTTGGGCATGTGGGC, *BamH*I; K78-F AGGTACC*AGGGGA*ACACGATGC, *Kpn*I). The amplified genes were cloned into pMMB-77 and pMMB-78 under *lac* promoter, which was then transformed to the *E. coli* DH5α as a heterologous host [13]. Recombinant enzymes 10*S*-DOX and 7,10-DS were produced in *E. coli* DH5α containing the plasmids pMMB-77 and pMMB-78,

respectively [13]. Recombinant *E. coli* DH5α/pMMB-10*S*-DOX and *E. coli* DH5α/pMMB-7,10-DS were grown in TSB supplemented with chloramphenicol (20 µg/mL) and incubated overnight at 30 ºC in a rotary shaker operating at 150 rpm. The cellular extract was obtained as follows: cells were collected by centrifugation at 10,000 xg for 20 min, 20-fold concentrated in 50 mM Tris-HCl buffer pH 7.0 and frozen at -20 °C. After thawing, ice jacketed, 1 mg/mL of lysozyme was added and sonicated at 70% vibration amplitude and 3 cycles of 1 min; 0.5 s pulse rate (Bandelin Sonopuls HD 3100). Clarified cell extracts were then recovered after ultracentrifugation at 40,000 xg, 30 min, 4 °C. Protease inhibitor cocktail cOmplete™, Mini, EDTA-free (Sigma-Aldrich) was used in the cellular extract samples. Finally, the samples were filtered twice with a centrifuge filter 30K molecular weight cutoff (15,000 xg, 30 min) in 50 mM Tris-HCl buffer pH 8.0.

2.5 Production of inclusion bodies

For the formation of IBs recombinant *E. coli* DH5α/pMMB-10*S*-DOX and *E. coli*, BL21/pEt28a-7,10-DS were grown in TSB supplemented with chloramphenicol (20 µg/ml) and protein production was induced during the exponential phase (O.D. 600 nm = 0.7) with 1 mM IPTG and 3 h of incubation at 37 ºC on a rotary shaker operating at 130 rpm. *E. coli* DH5α and *E. coli* BL21/pEt28a were used for negative-expression control. Thereafter, the centrifuged cells were resuspended in 20-fold volume in cellular lysis buffer (Tris-HCl buffer 50mM, pH 8.0, containing 100 mM NaCl and 1 mM EDTA) and frozen at -20 ºC. After thawing, the samples were ice-jacked and disrupted by sonication and centrifuged again (40 min, 15,000 xg). Then, the insoluble fraction including IBs was washed twice with the same volume of 50 mM Tris-HCl buffer at a pH of 8.0. Finally, the samples were filtered twice with a 30K molecular weight cutoff protein concentrator (30 min, 15,000 xg) using a double volume of 50 mM Tris-HCl buffer, pH 8.0.

2.6 Protein determination and SDS-PAGE molecular mass determination

Protein concentration was measured using the micro-volume spectrophotometer Thermo Scientific NanoDrop 2000 (Wilmington, DE, USA) and/or determined by the Bradford method using bovine serum albumin as the standard protein [24]. The estimated molecular mass of the recombinant proteins was determined by SDS-PAGE with resolving (10%) and (5%) stacking gels; standards and the samples were heated at 99 ºC for 5 min. Electrophoresis was performed at a constant current of 130v along with standard molecular mass markers Fermentas PageRuler™

Prestained protein ladder (SM0671, MW 10-170 kDa; Fisher Scientific, Walthman, MA, USA). After migration, gels were fixed, and proteins were stained with Coomassie Brilliant Blue following the procedure of Laemmli [25]. The content of the soluble recombinant proteins or IBs was determined by densitometric analysis of Coomassie-stained gels using a ChemiDoc XRS+ and Image Lab Software (Bio-Rad) imaging densitometer with bovine serum albumin (BSA) as the standard.

2.7 *In vitro* biotransformation assays

Fatty acids used as substrates were prepared from fresh stock solutions in 50 mM Tris-HCl buffer pH 7.0 with 2% DMSO or dimethyl sulfoxide >90% purity or in absolute ethanol and adjusted to the desired final concentration, 0.2 mM for OA and 0.8 mM for H(P)OME unless otherwise stated. Enzyme reaction comprised 500 µL of substrate solution, 100 µL of protein suspension (19.7 mg/mL for 10*S*-DOX or 27.0 mg/mL for 7,10-DS) and 400 µL of 50 mM Tris-HCl buffer pH 7.0. The reaction mixture was incubated (in a 2 mL Eppendorf tube) routinely for 20 min at 30 °C in a thermoblock (Labolan, Spain) with shaking at 750 rpm. The reaction was quenched by acidification to pH 2.0 with 0.5 M HCl. Products were extracted twice with ethyl acetate (1:1v/v) and strong vortexing. Organic phases were evaporated until dryness and recovered in methanol. Qualitative detection of fatty acid and oxylipins were performed in precoated TLC plates (0.25-mm Silica Gel 60A, 20 × 20 cm) (Macherey Nagel™ Aluminum Sheets Alugram SIL G), Phosphomolibdic acid hydrate (Fluka Analytical) 10% (w/v) in absolute ethanol (Panreac) as previously described using pure standards before LC analysis. All biotransformations were conducted under the same conditions, including a negative control, and all the assays were performed in triplicate. One unit of enzyme activity was defined as the amount of enzyme required for the conversion of 1 µmol of substrate per minute under the assay conditions used.

2.8 Substrate specificity

Substrate specificity for 10*S*-DOX was determined using 16:1 *cis*-9 (99%); methyl oleate (99%), 18:1 *cis*-9 (99%);18:1 *trans*-9 (99%), 18:1 *cis*-6 (99%); 18:1 *cis*-11 (99%); 18:1 *trans*-11 (99%); 18:2 (*cis*-9, 12) (99%); 18:3 (*cis*-6, 9, 12) (99%) and (12*S*)-HOME (99%) and 10-HOME (100%) as substrates (Table S1). Reaction products were identified by RP-LC-MS/MS analysis.

2.9 Biochemical characterization of 10*S*-DOX and 7,10-DS

Activity assays for 10*S*-DOX and 7,10-DS were carried out in 50 mM Tris-HCl, pH 7 buffer at 30 ºC or other temperatures as stated in the text, with the appropriate concentrations of substrates, OA or 10-H(P)OME respectively. The effect of pH on enzyme activity was determined in 20 mM Britton-Robinson buffer over a range of pH 5.0 to 10.0 at 30 ºC. The optimal temperature was also evaluated in standard assay conditions over a range of 20 °C to 50 °C at intervals of five degrees. Thermal stability was determined by incubating cell extracts in the corresponding buffer in sealed vials at different temperatures from 25 °C to 70 °C for 15 min. All the samples were immediately chilled in ice and the enzyme activity was measured under standard assay conditions at the optimum temperature. In each case, activity was expressed as a percentage of the maximum activity obtained at either optimum pH or optimum temperature.

The effect of divalent cations on enzyme activity was determined by the addition of the corresponding metal salts to the reaction mixture to obtain a solution with a final concentration of 1 mM. A 100 mM stock solution of the following compounds was used: $CoCl_2 \cdot 6H_2O$; $CdCl_2$; $NiCl_2 \cdot 6H_2O$; $HgCl_2$; $MnCl_2 \cdot 2H_2O$; $CaCl_2 \cdot 2H_2O$; $SnCl_2 \cdot 2H_2O$; $FeCl_2$; $MgCl_2 \cdot 6H_2O$; $ZnCl_2$; $CuCl_2 \cdot 6H_2O$. All compounds were dissolved in bi-distilled water, except $SnCl_2 \cdot 2H_2O$, which was diluted in 96% ethanol. Enzyme activity was measured by the RP-LC method. The residual activity was calculated and expressed as a percentage of the activity obtained in the absence of metal ions. Kinetic parameters were determined over a range of concentrations of OA (0.05 to 1.0 mM) and 10-H(P)OME (0.2 to 1.2 mM) at 30 ºC in 50 mM Tris-HCl, pH 7.0 buffer.

2.10 Determination of the active site metal

The active site metal of 10*S*-DOX and 7,10-DS was determined on an ICP-MS (inductively coupled plasma mass spectrometer), an AGILENT 7500ce model (Santa Clara, CA, USA). For the assay, 1 mL (3 μg/mL) of the sample was placed in a Teflon® reactor with 1 mL of HNO_3 (15 %) and 1 mL H_2O_2 for 48 hours at 90 °C, and then 22 mL of Milli-Q water was added.

2.11 Inclusion bodies purification

IBs purification was carried out following a modified protocol from Rodríguez-Carmona et al. [26]. Briefly, after thawing at -20 ºC, 1 mg/mL lysozyme was added to the bacterial suspension,

which was further incubated at 37 ºC at 130 rpm for 2 h. Triton X-100 0.5% was added, and incubation was continued at room temperature for 1 h. The mixture was disrupted by sonication with 4 to 6 cycles of 3 min (70% vibration amplitude and 0.5 s pulse rate). Samples were centrifuged (30 min, 15,000 x g) and the insoluble fraction was washed twice with the same volume in 50 mM Tris-HCl pH 8.0. Finally, samples were filtered twice with a 30K molecular weight cutoff protein concentrator (30 min, 15000 x g) in a double volume of 50 mM Tris-HCl buffer pH 8.0. After final filtration, purity was controlled by SDS-PAGE. Pure IBs were stored at -20 ºC. Protein concentration was measured using the micro-volume spectrophotometer Thermo Scientific NanoDrop 2000 (Wilmington, DE, USA) and/or determined by the Bradford method, using bovine serum albumin (BSA) as standard [24].

2.12 Determination of enzymatic activities of IBs

Catalytic activities of IBs-77 from *E. coli* DH5α/pMMB-77 and IBs-78 from *E. coli* BL21/pET28a-78 were determined. Protein concentration was 192 µg/mL and 257 µg/mL for IBs-77 and IBs-78, respectively. Enzymatic assays were performed with 0.1 mL of enzyme preparation incubated with the appropriate substrate solution. Specifically, for the *PA2077* enzyme 20 mM of OA (Sigma Aldrich) and *PA2078* 1.6 mM 10-H(P)OME were prepared in 50 mM Tris HCl pH 7.0. Reaction conditions are described in section 2.7.

2.13 Liquid chromatography analysis

Quantification of the enzymatic activity was determined by RP-LC (reverse-phase liquid chromatography), quantifying the amount of reduction of the substrate compared with the control without enzyme. Analysis was carried out using a Shimadzu LC-9A chromatograph (Shimadzu, Japan), with a Tracer Exel column 120 C8 (150 mm × 4.6 mm, 5 µm) (Teknokroma, Spain) coupled to a Sedex 55 light-scattering detector (Sedere, France). Optimal separation was achieved with a gradient elution using A: acetonitrile (0.1% v/v acetic acid) and B: water (0.1% v/v acetic acid) at the flow rate of 1 ml/min or 2.5 ml/min and a gradient (min, %A): (0, 50), (15, 100), (25, 100), (27.5, 50), (30, 50). The volume of injection was 50 µL. Retention times of fatty acid and hydroxylated fatty acid were established using a home standard.

2.14 Proteolytic digestion

Fresh pure IBs were treated following a reported methodology [27]. Briefly, IBs were suspended in PBS pH 8.0 and sonicated to obtain a homogeneous suspension before diluting to 1.0 optical density (OD) 350 nm. Proteolytic digestion of IBs was induced by adding 0.02 mg/mL of proteinase K (PK) and incubated at 25 ºC with gentle shaking for 30 min. A control suspension in PBS without PK was performed under the same conditions. Proteolytic digestion was monitored by collecting samples every 7 min. When necessary, phenylmethylsulfonyl fluoride PMSF (Sigma) 1 mM was added to inhibit digestion. Digested IBs samples were visualised by SDS-PAGE.

2.15 Amyloid specific dye-binding assays for IBs

Congo Red (CR) binding was determined by the spectroscopic band shift assay using a Shimadzu UV/1800 spectrophotometer (Kyoto, Japan) in the range of 400 to 650 nm using quartz cuvettes (10 mm light path). Samples (1 mL) containing 20 µg/mL of the corresponding IBs-77 or IBs-78 and CR (10 µmol) were incubated in PBS for 30 minutes [27]. Solutions of dye in the absence of protein and protein samples in the absence of dye were used as negative controls in the dye-IB interaction analysis. The binding of Thioflavin-T (Th-T) to IBs (20 µg/mL) was determined in PBS containing 65 µmol Th-T and 0.02 mg/mL PK, adjusted to a final volume of 1 mL in a 10 mm quartz cuvette. The fluorescence emission spectra of samples were recorded for 30 min, using an excitation wavelength of 440 nm at 25 °C, on a Spectronic Unicam AB2 Luminescence Spectrofluorimeter [28].

2.16 Fourier Transform Infrared Spectroscopy (FT-IR)

For FT-IR spectroscopy analysis, purified samples of IBs and control cell pellets were suspended in distilled water and lyophilised (Telstar Cryodos) before analysis to reduce water interference in the infrared spectra. The FT-IR spectra of the dry samples were analysed using a Nicolet 6700 Thermo Scientific FT-IR spectrometer. Spectra were recorded from approximately 3500 to 600 cm^{-1}. A second derivative was used (see Results below) to precisely establish the band minima. The amide bands were present in the spectral range of 1500-1700 cm^{-1} used for the analysis of aggregates and secondary structures in proteins such as β-sheets, α-helix, and others. The background spectrum was collected before each measurement.

2.17 Atomic force microscopy (AFM)

Purified IBs (5-10 µL) were suspended in sterilised bi-distilled water at a protein concentration of 20-25 µg/mL. A drop of the suspension was deposited onto freshly cleaved mica or glass coverslips. The samples were blow-dried with nitrogen after adsorption at room temperature. AFM studies were conducted in air at room temperature using an extended multimode AFM head with a Nanoscope controller (Bruker, Germany). All images were recorded in peak force tapping mode with triangular SNL silicon cantilevers (normal radius of 6-8 nm) at a scan rate of 1 Hz.

2.18 LC-MS/MS analysis

RP-LC MS/MS analysis was performed with a quaternary MS pump system from the Accela model (Thermo Scientific) and with an analytical silica column Tracer Excel 120 C8 column (150 mm × 4.6 mm, 5 µm) (Teknokroma, Spain), which was eluted usually at a flow-rate of 0.6 mL min^{-1} with A: acetonitrile (0.1% v/v acetic acid), B: water (0.1% v/v acetic acid). The eluent was exposed to electrospray (ESI) for monitoring negative ions in an LTQ-Orbitrap (Thermo Scientific) ion mass spectrometer. The electrospray voltage was set at 3.5 kV and the temperature of the heated capillary was set at 400 °C. Data acquisition was performed using Xcalibur software (Thermo Scientific) while the identification of compounds was performed as previously described [13].

2.19 Screening for oxylipin-producer bacteria

In order to detect new prokaryotes with diol-synthase activity bacteria belonging to the genera *Aeromonas, Shewanella, Thauera, Ensifer* and other *Pseudomonas* than *P. aeruginosa* were screened: *Aeromonas allosaccharophila* CECT 4220, *Aeromonas bivalvium* 868E, *Aeromonas caviae* CECT 4226, *Aeromonas hydrophila* CECT 839, *Aeromonas salmonicida* CECT 894, *Pseudoalteromonas antarctica* DSM151318, *Pseudomonas tolassi* ATCC 33618, *Pseudomonas fluorescens* CECT 844, *Pseudomonas fragi* DSM 3456, *Pseudomonas lini* DSM 16768, *Pseudomonas lundensis* DSM 6252, *Pseudomonas taetrolens* DSM 21104, *Shewanella vesiculosa* CECT 7339, *Shewanella putrefaciens* ATCC 8071; all strains incubated at 30 °C except *S. vesiculosa* at 20 °C in TSB (g/L): casein peptone (17), soymeal peptone (3), glucose (2.5), NaCl (5), KH_2PO_4 (2.5). *Pseudoalteromonas aliena* DSM16473, *Pseudoalteromonas atlantica* CECT 579, *Shewanella hanedai* ATCC 33224, were incubated at 20 °C (except *Shewanella. woodiy* at 30 ºC) in Marine broth (MB) medium (g/L): Peptone (5), Yeast extract (1), iron (III) citrate (0.1), NaCl

(19.45), $MgCl_2$ (5.9), $MgSO_4$ (3.24), $CaCl_2$ (1.8), KCl (0.55), $NaHCO_3$ (0.16), KBr (0.08). After autoclaving, the following solution was added to the following final concentration (mg/L): Vitamin B12 or cyanocobalamin (0.5), Thiamine hydrochloride (0.4) and biotin (0.4) and when convenient agar 15g/L was added. *Ensifer fredii* DSM 5924 was incubated at 30 ºC in TY medium (g/L): Tryptone (5.0), Yeast extract (3.0), $CaCl_2 \cdot 6$ H2O (1.3) and when convenient agar 15 g/L was added. *Thauera aminoaromatica* DSM 25461 was incubated at 30 ºC in Stoke's medium (g/L): Polypeptone (5), $MgSO_4 \cdot 7H_2O$ (0.2), $FeNH_4SO_4$ (0.15), Sodium citrate (0.1), $CaCl_2$ (0.05), $MnSO_4$ (0.05) and $FeCl_3 \cdot 6H_2O$ (0.01) supplemented with 15 g/L of Bacto agar when convenient.

The bacterial cultures preserved at -80 °C were grown in 50 mL at their suitable conditions for 24 h or 48h. After grown, cells were harvested and centrifuged at 10000 x g for 30 min; the pellet was sonicated and the cell extract was clarified as previously described in section 2.7. The cellular extract was incubated at pH 7.0 with 0.5-1% of OA for 30 min at 30 ºC and 150 rpm. Products were produced and analyzed as described in the "Biotransformation assay" section.

2.20 Statistical analysis and reproducibility

All determinations of enzyme activity were performed in triplicate and represented values correspond to the average ± standard deviation.

3. Results

3.1 Expression of the recombinant enzymes

As stated in the Material and Methods Section, the recombinant strain of *E. coli* DH5α bearing pMMB-77 or plasmid construction pMMB-78 was used for enzyme characterization. The effect of substrate and enzyme concentration was determined in previous assays (results not shown) to establish the conditions of the forthcoming assays. The 10*S*-DOX was established at 0.20 mM of OA and enzyme at 1.97 mg protein/100 µL, whereas the 7,10-DS substrate (10-H(P)OME) was determined at 0.8 mM and enzyme at 2.70 mg protein /100 µL.

3.2 Substrate specificity of 10*S*-DOX

Substrate specificity was determined using various unsaturated fatty acids as presented in Table S1. The OA preference was confirmed as previously reported as depicted in Fig. 2 [15]. Ricinoleic acid (12-HOME) was the second preferred substrate with 87.6% relative activity compared with OA control. Substrates with double bonds in position C9/C12 reflected a higher yield of transformation than other assayed substrates, which rendered more than 45% of activity reduction. Furthermore, neither the *cis/trans* configuration; the position of the double bond (C9-C11-C12) and the methyl group in methyl oleate nor the polyunsaturation in linoleic acid was an impediment to enzyme conversion. OA, being the preferential substrate, was used for further characterisation assays of the 10*S*-DOX enzyme and the production of 10-H(P)OME required for the biochemical characterization of the 7,10-DS enzyme.

3.3 Production of 10*S*-H(P)OME, the substrate of 7,10-DS

The substrate for 7,10-DS, 10-H(P)OME was produced *"in vitro"* using *P. putida* KT2440/pBB-77 producing 10*S*-DOX. After DNA extraction, the fragment containing PA-2077 was subcloned into a pMMB vector and then transformed into a *P. putida* KT2440 (see materials and methods section). Maximum 10-H(P)OME rates were achieved with 0.5 g/L of OA and were used for monitoring the bioconversion of OA. The 10-H(P)OME relative concentration increased steadily from 20 min; a 91% (w/w) conversion yield was achieved at this time: 73% of 10*S*-H(P)HOME and 18.0% were spontaneously reduced to 10*S*-HOME with 9% of remained OA (Fig 3). *P. putida* KT2440 was evaluated for 10-H(P)OME, 10-HOME and 7,10-DiHOME production by biotransformation assays of OA and home-produced 10-H(P)OME as a negative control of the presence of 10*S*-DOX and 7,10-DS or other oleate-derived oxylipin-forming enzymes.

3.4 Molecular weight and active site metal ion

The mass range was determined by SDS-PAGE after purification, with standard molecular mass markers (molecular mass 10 to 170 kDa). Gels were fixed and proteins were stained with Coomassie Brilliant Blue R-250 after migration. The molecular weight was estimated as 66.73 kDa and 65.89 kDa for 10*S*-DOX and 7,10-DS, respectively (Fig. S1). Inductively coupled plasma mass spectrometry indicated that both 10*S*-DOX and 7,10-DS contained Fe^{2+} bound to the heme group as a prosthetic group in a concentration of 0.95 mol of Fe^{2+} per mol of protein (10*S*-DOX) and 1.18 mol of Fe^{2+} per mol of protein (7,10-DS).

3.5 Biochemical characterization of 10*S*-DOX and 7,10-DS

Expression assays of *E. coli* DH5α/pMMB-10*S*-DOX and *E. coli* DH5α/pMMB-7,10-DS were performed at 30 ºC for 15 min in a 50 mM Tris-HC buffer, pH 7 or otherwise as stated in the text.

The effect of pH on enzyme activity was determined at 30 ºC (Fig. 4). Britton-Robinson buffer adjusted at different pH (3-10) was used for optimum pH determination. Both 10*S*-DOX and 7,10-DS displayed the same pH profile of relative activities as the maximum activity occurred in a wide pH range from neutral to basic (pH 7.0 to 10.0).

The effect of temperature was evaluated in the range of 20 to 50 ºC for both enzymes, whereas the optimal temperature was similar for both enzymes: 30 ºC for 10*S*-DOX and 35 ºC for 7,10-DS as presented in Fig. 5. Nevertheless, 10*S*-DOX activity presented a high marked peak while 7,10-DS revealed a platform in the range of 35 to 40 ºC. The thermostability assays were performed at pH 7.0 by quantifying the residual enzyme activity upon pre-incubation of the protein solution at temperatures ranging from 25 to 60 ºC for 10 min (Fig. 6). Both enzymes were unstable over 50 ºC and lost about 50% of the activity (10*S*-DOX = 49.2% and 7,10-DS = 54.8%) when they were incubated for 15 min at 30 ºC. The 7,10-DS enzyme was more thermostable than 10*S*-DOX, especially when the enzyme was incubated for 15 min at 25 ºC. The complete inactivation of oleate-diol synthase enzymes occurred at 60 ºC.

The influence of different divalent cations on enzyme activity is presented in Figure 7: 10*S*-DOX in the presence of Co^{2+}, Hg^{2+} or Zn^{2+} retained 93.3%, 89.1% and 86.7% respectively of its total activity, followed by 78.6% of Ca^{2+}, 73.42% of Mg^{2+} or 70.27% Ni^{2+}. Enzyme activity was halved in the presence of Fe^{2+}, Mn^{2+}: 61.84% and 51.6%, respectively, and reduced to 39.9% in the presence of Sn^{2+}.

For 7,10-DS, the activity was enhanced (%) in the presence of Mg^{2+} (127.81), Sn^{2+} (109.53), Cd^{2+} (103.22). Meanwhile, the enzyme was barely affected in the presence of Co^{2+} or Fe^{2+} as the values were 93.2% and 92.7%, respectively. In the case of Ca^{2+}, the remaining activity was 86.42% while the addition of Hg^{2+} decreased the enzyme activity to 54.9% (Fig 7).

The kinetic parameters of both enzymes were determined under suitable conditions of pH and temperature. Specifically, 10*S*-DOX was obtained from clarified cell extracts from *E. coli* DH5α/pMMB-77 and the activity was determined at different OA concentrations from 0.05 to 0.35 mM, whereas 10*S*-DOX displayed a substrate inhibition profile up to 0.35 mM of OA and enzyme activity decreased more than 50% (data not shown). The K_M and V_{max} for 10*S*-DOX were obtained

directly from the linearisation of the Lineweaver-Burk equation and their values were 0.89 ± 0.22 mM and 14.7 ± 0.26 U g^{-1} min^{-1}, respectively (Fig. 8a).

For 7,10-DS obtained from *E. coli* DH5α/pMMB-78, the activity was determined at different substrate concentrations of (10*S*-H(P)OME) in the range of 0.2 to 1.2 mM. The kinetic parameters determined from Lineweaver-Burk equation plots were K_M of 3.26 ± 0.31 mM and V_{max} of 54 ± 0.38 U g^{-1} min^{-1} (Fig. 8b).

3.6 Detection and characterisation of inclusion bodies

Among the clones constructed in this study, it was found that *E. coli* DH5α, bearing pMMB-77 and *E. coli* BL21/pET28a-78 produced inclusion bodies, IBs-77 and IBs-78, respectively. The amount of IBs obtained using *E. coli* DH5α/pMMB-77 (IBs-77) was 6 mg/mL, which constituted 76.9% of the total cellular protein production (Table S2). In the case of *E. coli* BL21/pET28a-78 (IBs-78), 6.4 mg/mL of crude IBs was produced, accounting for 75.3 % of the total protein. The electrophoretic analysis demonstrated crude IBs with a small proportion of other peptides (Fig. S2, lanes 1 and 3). After the purification process, concentrations of 2.2 mg/ml and 3.2 mg/ml were obtained for IBs-77 and IBs-78, corresponding to the purification degrees of 4.6 and 6.9, respectively (Fig. S2, lanes 2 and 4). Thus, the final amount of pure IBs in the total cellular protein content was 11.15% for 77 (10*S*-DOX) and 16.31% for 7.8 (7,10-DS).

The specific activity of the soluble fraction after bacterial sonication was negligible in both cases (0.8 x 10^{-3} IU/mg). Crude IBs specific activity was 1.55 IU/mg in IBs-77 and 1.0 IU/mg in IBs-78. Pure IBs-77 specific enzyme activity was reduced to 1.0 IU/mg during the purification process, whereas that of pure IBs-78 increased to 2.2 IU/mg.

3.7 Determination of inclusion body structure/architecture

FT-IR spectroscopy constitutes an easy and rapid method for the characterisation of IBs protein structure and determining high levels of the intermolecular β-sheet structures characteristic of amyloid fibrils. Purified IBs and cell pellets were lyophilised before the analysis to reduce water interference in the infrared spectra and the background spectrum was collected before each measurement. The FT-IR spectra of IBs-77 and IBs-78 are characterised by two main band components around 1654 cm^{-1} and 1629 cm^{-1} in the Amide I region, which can be respectively

assigned to α-helix and β-sheet structures of the protein [30]. The component at 1621 cm^{-1} indicates that the polypeptide backbones involved in the β-sheet assembly are tightly packed and shared short hydrogen bonds. The FT-IR spectra of both native (soluble) proteins revealed small peaks at 1623 and 1628 cm^{-1} assignable to β-sheets (Fig 9a, Fig. 9f), indicating the formation of IB aggregates led to a small increase in β–sheets and a decrease in α-helix. Th-T binding assays were determined as changes in the fluorescence emission spectra, with a maximum emission from 445 nm to 482 nm due to the dye bound to IBs (Fig S3).

3.8 Proteolytic digestion

An insight into the fine structure of IBs-77 and IBs-78 was obtained by PK digestion. As IBs are aggregate proteins of amyloid structure with misfolded proteins of other protein species, PK digestion might reveal the heterogenicity of the aggregates. As soon as PK was added to the protein suspension, a sharp decrease in turbidity was observed due to the proteolysis of the particles (Fig S4 4 a, b). In the case of IBs-77, 35% of protein remained PK-resistant at the end of the digestion and the initial specific activity decreased sharply from 0.685 IU/mg to 0.151 IU/mg after 10 min (77%) and to 0.023 IU/mg at the end of the experiment (96.6%). In contrast, the decline in turbidity in IBs-78 was gradual, suggesting a different type of IBs, although similar resistance (32%) to solubilisation was observed at the end of the digestion. Likewise, the decrease in enzyme activity was similar to IBs-77, increasing from 0.800 IU/mg to 0.175 IU/mg after 10 min (78% loss) and to 0.027 IU/mg at the end of the experiment (96.6% loss).

3.9 Atomic Force microscopy

Atomic Force Microscopy (AFM) proved to be a useful technique for exploring the morphology of the IBs. On a graphite surface, the cantilever of AFM images depicts the appearance of the aggregates before (Fig 10A) and after 30 min of PK digestion. In the background, fibrils released from the nucleus of the particles can be seen (Fig. 10B white arrows) together with irregular material, the scaffold of the PK-resistant aggregates. IBs-77 aggregates demonstrated an irregular structure after PK digestion, which decreased by ca. 61-65% and ca. 69-83% for IBs-78.

3.10 Screening for 10*S*-DOX and 7, 10-DS activities in other proteobacteria

Different species of environmental proteobacteria belonging to 6 genera with similar habitats: water, soil and plant interaction were tested using OA as a substrate to explore diol synthase activity in the bacterial kingdom. In addition, multiple amino acid sequence alignments of *PA2077* and *PA2078* among these six genera could present similar consensus motifs such as conserved two heme sequences (CXXCH) that are responsible for covalent attachment in bacterial di-heme cytochrome c peroxidases, ferrous ion union (EGR), P450 motifs (EXXR), and the essential histidine of oxidases (MauG). Some of the bacteria screened were selected based on the phylogenetic proximity with *P. aeruginosa* and others have previously given positive distant matches (*T. aminoaromatica* and *E. fredii*) [13].

After growing selected bacterial strains under suitable conditions (see material and methods section), analysis of the organic extract by LC-MS/MS revealed that these bacteria have the putative ability to produce the same oxylipins (10-H(P)OME and 7,10-DiHOME) from OA as found in *P. aeruginosa*. Briefly, after a full scan of the total ion current (TIC) from *m/z* 100-800, MS^2 analysis *m/z* 297.2 and *m/z* 313.2, and MS^3 analysis (*m/z* 313.2→*m/z* 295.2) were selected for 10-H(P)OME (Fig S5 a, b) and 7,10-DiHOME (Fig S6 a, b) discrimination (Fig S5 a, b; S6 a, b).

Table II presents the first report of bacterial strains assayed to detect the diol synthase pathway. As observed in most of the bacteria assayed, 10*S*-hydroxy-8*E*-octadecenoic acid (10-HOME) was detected. This product is a side compound from the spontaneous reduction of 10-H(P)OME in *P. putida*, *Pseudomonas. psycrophyla* and *Pseudomonas. oleovorans* but could not transform OA into the selected oxylipins despite grown under suitable conditions.

Using *P. aeruginosa* as a positive control, the activity of 10*S*-DOX and 7,10-DS was determined by analysing the released product. The MS^2 spectrum of 10-H(P)OME from the OA conversion produced signals at *m/z* 155.279 and the MS^3 spectrum of 10-H(P)OME gave predominant signals at *m/z* 155.179; 251.277 (Fig. S5. a, b). The corresponding ions of 7,10-DiHOME obtained from the conversion of 10-H(P)OME from MS^2 spectra were found at *m/z* 251, 293, 295, and 314 and prominent signals from the 7,10-DiHOME MS^3 spectrum were found at *m/z* 155, 179, 251 and 277 (Fig. S6. a, b).

Diol synthase activity was also found in other species of *Pseudomonas.* When the cell extract of *P. tolassi, P. lini* or *P. fluorescens*, was incubated with OA (30 min), analysis of the products by LC-MS/MS revealed the presence of 10-H(P)OME and 7,10-DiHOME in the supernatant, suggesting the presence of functional proteins of 10*S*-DOX and 7,10-diol synthase (7,10-DS) (Fig. S7. a, b).

Several species of *Aeromonas* were also screened for diol synthase activity. Cellular extracts of *A. allosaccharophila, A. bivalvium, A. caviae,* and *A. salmonicida* were incubated with OA for 30 minutes, and two oxylipins derived from OA, 10-H(P)OME and 7,10-DiHOME were detected in the supernatant. The corresponding spectra are shown in Fig. S8 (a, b). In the supernatant of *A. hydrophila* and *Aeromonas. allosacchariphila,* only 7,10-DiHOME was detected, although there were indications that the complete functional diol synthase system was present since as stated earlier the substrate for 7,10-DS is the product of the first reaction catalysed by 10*S*-DOX. A different range of products was found when assaying species of *Shewanella* (Fig. S9 a, b) cell extracts of *E. fredii* (Fig. S10. a, b) incubated with OA as both H(P)OME and 7,10-DiHOME were detected.

It has been reported that the diol-synthase activity might have evolved from a common ancestor (orthologs) or by lineage-specific duplication (in paralogs). It was predicted that in the β-proteobacteria, *T. aminoaromatica,* and the α-proteobacteria, *E. fredii,* a similar relation to the ORF *PA2078-PA2077* of *P. aeruginosa* (a γ-proteobacteria) was detected [13].

4. Discussion

Hydroxy-fatty acids are common constituents in plants, animals and fungi. The endogenous hydroxy fatty acids are the consequence of the activity of different enzymes: hydratases, P450 monooxygenases, lipoxygenases, and diol synthases [31]. DOX activity was first found in *Laetisaria arvalis* as a fungicidal metabolite formed from linoleic acid [32]. Thereafter, its mechanism of action was described in 1993 and the metabolite was fully identified as 8*R*-hydroxylinoleic acid [33]. The combined action of diol synthase and hydroperoxide isomerase in polyunsaturated fatty acids was found in *Gaeumannomyces graminis* rendering 7*S*,8*S*-dihydroxy-9*Z*,12*Z* octadecadienoic acid as a tetrameric protein [34,35]. Later, DOX activity was identified in *Aspergillus,* the metabolic pathway was biochemically characterised as a single enzymatic activity [36]. Meanwhile, a bifunctional enzyme, a linoleate diol synthase activity on polyunsaturated fatty acids were reported in the bacteria: Cyanobacteria *Nostoc* [37].

The discovery of the genes involved in OA metabolism in *P. aeruginosa* demonstrated that two different enzymes acting sequentially 10*S*-DOX encoded by *PA2077* and 7,10-DS encoded by *PA2078,* were responsible for diol synthase activity and the enzymes were classified in the

FadCCPs subfamily [13]. Fatty acid oxygenases are important due to their physiological role and their use in green chemistry for sustainable industrial processes but FadCCPs have remained uncharacterised to date.

Here, we demonstrated that the first acting enzyme, 10*S*-DOX, has a wider range of substrates than previously reported [38]. Although OA is the preferred substrate, ricinoleic acid can be bioconverted to (10*S*,12*R*)-dihydro(per)oxy-(8*E*)-octadecenoic acid with an 88% of the relative activity compared with OA together with other substrates. Furthermore, the affinity with linoleic acid was 42%, indicating that the new enzyme differs from the cyanobacterial diol synthase previously reported [37].

We have designed and optimised the production of 10-H(P)OME with *P. putida* KT2440/pBBR-77 and employed it for *in vitro* production, achieving high yields of 71.4%, w/w after 1 h of incubation. This is the first report on the production of 10-H(P)OME, particularly in a case where is used as the substrate for 7,10-DS synthesis. *P. putida* KT2440 might be a promising microorganism host for 10*S*-DOX functional production for biotechnological purposes, which requires high conversion yields, mild temperatures and shorter bioconversion rates for the production of hydroperoxide derived from a broad range of long-chain fatty acids as shown above. However, the 10-H(P)OME produced by the *P. aeruginosa* ΔDS/pBBR-77 was lower (33.0%). This finding might be due to the cellular redox environment of the extract of *P. putida* KT2440, which allows higher stability of the 10-H(P)OME than in the homologous host.

The biochemical characterisation of the enzymes, 10*S*-DOX and 7,10-DS, involved in the oleate-diol synthase pathway demonstrated similar pH profiles. This might be attributed to their localisation in the same cellular compartment. Meanwhile, 10*S*-DOX presented its highest activity at 30 ºC while 7,10-DS did not show a clear preferred temperature. These differences were also reflected in the thermostability assays. The thermal instability in 10*S*-DOX and 7,10-DS enzymes could be due to their nature as intracellular enzymes, which have evolved to be active at cellular temperatures in mesophilic hosts such as *P. aeruginosa.* The effect of divalent ions in reaction media is different for both enzymes.

The enzymatic activity of 10*S*-DOX (IBs-77) and 7,10-DS (IBs-78) reflects that the protein inactivation during *in vivo* protein aggregation is only moderate and aggregation does not necessarily compromise the active centre of the enzyme as it has been previously reported for other bacterial enzymes [38]. From the structural point of view, the catalytic activity found in IBs depends on the kinetics of the aggregate formation and the nature of the protein. IBs consist partly

of misfolded protein and partly of properly folded protein trapped in the hydrophobic network formed by the aggregate polypeptides [39].

An interesting tool for the study of the IB structure is FT-IR spectroscopy, which provides molecular insight into the aggregated protein. In this context, the most interesting region of the IR spectra in the amide I band or the self-deconvoluted spectra avoids the noise of the second derivative spectra [40]. This band essentially corresponds to the absorption of the carbonyl peptide bond group of the main protein chain and is therefore a sensitive marker of the protein secondary structure. The presence and relative position of the amide I and amide II bands are generally used to determine the cross-β-structure of most amyloid fibrils [41]. The most relevant band for assessing the amyloid structure of IBs by FT-IR was Amide I of the second derivative spectra, a predominant band of the protein infrared spectrum [41]. The amyloid structure is frequently found in IBs in prokaryote and eukaryote cells and the results reported in the present study are consistent with previous research [27,28,30,38,42–44].

Th-T binding indicates the presence of amyloid fibrils. The broad specificity of this endolytic serine protease has been employed in mapping polypeptide regions in the core of amyloid fibrils, due to its strong preference for hydrolysing unstructured protein regions [45]. IBs-77 and IBs-78 in the presence of Proteinase K (PK) treatment modified the emission of Th-T used to assess the amyloid structure of the proteins (Fig S3). These results were confirmed by Congo Red binding assay results (not shown) [46]. After PK was added to the protein suspension to digest the aggregates, a resistant fraction of protein found during PK incubation was visualised by SDS-PAGE. The data obtained indicated different classes of polypeptides were trapped within the IBs.

AFM was used to investigate the morphology of IBs-77 and IBs-78 pre-and post-PK digestion (Fig. 10). As expected, released fibrils were visible in both cases post-digestion (Fig.10, white arrows), and the remaining material corresponded to the scaffold of the aggregates. Similar results have been reported in previous studies [41,43,47].

Diol-synthase activity in bacteria was not restricted to the species *P. aeruginosa*. All the species assayed from the genus *Aeromonas, Pseudoalteromonas, Shewanella* and *Pseudomonas* belong to the class of γ-proteobacteria and they share similar habitats and conditions. The other two β-proteobacteria *E. fredii* and *T. aminoaromatica* were selected given that a previous report predicted that they share the tandem *PA2077-PA2078* in *Thauera* (tmz1t2187-tmz1t2188) and *Azoarcus/Ensifer* (azo2594-azo2595) both genus belong to β-proteobacteria). The phylogenetic tree of orthologous diol synthase-encoding genes present in *P. aeruginosa* revealed that the diol

synthase operon could be due to a gene duplication event in a common ancestor maintaining an adjacent location, although one of the genes evolved a new function [13,48]. A similar disposition of related genes has been described in cyanobacteria: a cyclooxygenase (10*S*-dioxygenase) that works in tandem with a catalase-related protein, rendering 10*S*-hydroperoxide lyase activity [49] and a bifunctional enzyme, a lipoxygenase with diol synthase activity from the cyanobacteria *Nostoc*, generating (10*E*,12*E*)-(9,14) dihydroxy-(10,12)-octadecenoic acid from linoleic acid [37].

This study characterises two novel FadCCPs enzymes: 10*S*-dioxygenase and the 7*S*,10*S*-diol synthase involved in oxylipin formation. To date, this is the first report of biotechnology production of 10-H(P)OME to be achieved in a new recombinant strain of *P. putida* KT2440/pPBR-77. The occurrence of active IBs of the enzymes of the diol-synthase pathway might be a great advantage for *in vitro* catalysis production of hydroxyl fatty acids for biotechnological applications.

An experimental screening was performed to display if other proteobacteria can produce H(P)OME and DiHOME in the presence of OA based on phylogenetic proximity to *P. aeruginosa*. The screening demonstrated the presence of an enzymatic system producing the same hydroxyl-fatty acids as the oleate diol synthase pathway first described in *P. aeruginosa*. The enzymatic system comprised two single enzymes, 10*S*-DOX which catalyse OA into 10*S*-hydroperoxid-8*E*-octadecenoic acid 10-H(P)OME and a second enzyme a 7,10 (D,S) Diol synthase converting the hydroperoxide H(P)OME into 7,10-DiHOME. It has been demonstrated in the genera *Pseudoalteromonas, Shewanella, Aeromonas, Ensifer,* and *Thauera* that the presence of a putative diol synthase system is not restricted to *P. aeruginosa* as earlier described.

ACKNOWLEDGEMENTS

We are grateful to P. Diaz. Faculty of Biology, University of Barcelona for her collaboration in the project. We thank the Scientific and Technological Centers of the University of Barcelona (CCiTUB) for technical support in LC/MS. This work has been funded by the Ministerio de Economía y Competitividad CTQ2014-59632-R (2014-2017) and by the Generalitat de Catalunya project 2017 SGR30.

REFERENCES

[1] A.R. Brash, Lipoxygenases: occurrence, functions, catalysis, and acquisition of substrate, J. Biol. Chem. 274 (1999) 23679–82, https://doi.org/10.1074/jbc.274.34.23679.

[2] E.H. Oliw, Linoleate diol synthase related enzymes of the human pathogens *Histoplasma capsulatum* and *Blastomyces dermatitidis*, Arch. Biochem. Biophys. 696 (2020) 108669, https://doi.org/10.1016/j.abb.2020.108669.

[3] Y.C. Joo, D.K. Oh, Lipoxygenases: Potential starting biocatalysts for the synthesis of signaling compounds, Biotechnol. Adv. 30 (2012) 1524–1532, https://doi.org/10.1016/j.biotechadv.2012.04.004.

[4] K.Y. Chen, I.H. Kim, C.T. Hou, Y. Watanabe, H.R Kim, Monoacylglycerol of 7,10-Dihydroxy-8(E)-octadecenoic acid enhances antibacterial activities against food-borne bacteria, J. Agric. Food Chem. 67 (2019) 8191−8196, https://doi.org/10.1021/acs.jafc.9b03063.

[5] H.T. Hou, Biotechnology for fats and oils: new oxygenated fatty acids, New Biotechnol. 26 (2009) 2–10, https://doi.org/10.1016/j.nbt.2009.05.001.

[6] K.C. Shin, M.J. Seo, J.H. Ju, D.K. Oh, Production of 6,8-dihydroxy fatty acids by recombinant *Escherichia coli* expressing T879A variant 6,8-linoleate diol synthase from *Penicillium oxalicum*, J. Am. Oil Chem. Soc. 96 (2019) 663-669, https://doi.org/10.1002/aocs.12219.

[7] H.M. Kim, H.R. Kim, H.T. Hou, B.S. Kim, Biodegradable photo-crosslinked thin polymer networks based on vegetable oil hydroxy fatty acids, J. Am. Oil Chem. Soc. 87 (2010) 1451-1459, http://dx.doi.org/10.1007/s11746-010-1634-6.

[8] I. Martín-Arjol, T.A. Isbell, A. Manresa, Mono-Estolide Synthesis from trans-8-Hydroxy-Fatty Acids by Lipases in solvent-free media and their physical properties, J. Am. Oil. Chem. Soc. 92 (2015)1125-1141, https://doi.org/10.13140/RG.2.1.1700.2089.

[9] A. Adrio, J.L. Demain, Microbial enzymes: Tools for biotechnological processes, Biomolecules. 4 (2014), 117–139, https://doi.org/10.3390/biom4010117.

[10] T. K. Tran, P. Kumar, H.R. Kim, C.T. Hou, B.S. Kim, Microbial conversion of vegetable oil to hydroxy fatty acid and its application to bio-based polyurethane synthesis, Polymers 10 (2018) 927, https://doi:10.3390/polym10080927.

[11] S.G. Burton, Oxidizing enzymes as biocatalysts, Trends Biotechnol. 21 (2003) 543–549, https://doi.org/10.1016/j.tibtech.2003.10.006.

[12] A. Garreta, X. Carpena, M. Busquets, M.C. Fusté, I. Fita, A. Manresa, Crystallization and resolution of the lipoxygenase of *Pseudomonas aeruginosa* 42A2 a phylogenetic study of the subfamilies of the lipoxygenases, in: D.M. Torrero (Ed.), Recent Adv. Pharm. Sci., Transworld Research Network, Kerala, India, 2011, pp. 249–273, http://hdl.handle.net/2445/21364.

[13] M. Estupiñán, P. Diaz, A. Manresa, Unveiling the genes responsible for the unique Pseudomonas aeruginosa oleate-diol synthase activity, Biochim. Biophys. Acta. 1841 (2014) 1360–1371, https://doi.org/10.1016/j.bbalip.2014.06.010.

[14] M. Estupiñán, D. Álvarez-García, X. Barril, P. Diaz, A. Manresa, in silico/in vivo insights into the functional and evolutionary pathway of Pseudomonas aeruginosa oleate-diol synthase discovery of a new bacterial di-Heme cytochrome C peroxidase subfamily, PLoS One. 10 (2015) e0131462, https://doi.org/10.1371/journal.pone.0131462.

[15] E. Martinez, M. Hamberg, M. Busquets, P. Díaz, A. Manresa, E. Oliw, Biochemical characterization of the oxygenation of unsaturated fatty acids by the diogenase and hydroperoxide isomerase of *Pseudomonas* 42A2, J. Biol .Chem. 285 (2010) 9339-9345, https://doi.org/10.1074/jbc.m109.078147.

[16] E. Martínez, M. Estupiñán, F.I.J. Pastor, M. Busquets, P. Díaz, A. Manresa, Functional characterization of ExFadLO, an outer membrane protein required for exporting oxygenated long-chain fatty acids in *Pseudomonas aeruginosa*, Biochimie 95 (2013) 290–298, https://doi.org/10.1016/j.biochi.2012.09.032.

[17] A. Singh, V. Upadhyay, A.K. Upadhyay, S.M. Singh, A.K. Panda, Protein recovery from inclusion bodies of *Escherichia coli* using mild solubilization process, Microb Cell Fact. 14 (2015) 41, https://doi.org/10.1186/s12934-015-0222-8.

[18] D. Jamrichová, L. Tišáková, V. Jarábková, A. Godány, How to approach heterogeneous protein expression for biotechnological use: An overview, Nova Biotechnologica et Chimica. 16 (2017) 1–11, https://doi.org/10.1515/nbec-2017-0001.

[19] C. Slouka, J. Kopp, O. Spadiut, C. Herwig, Perspectives of inclusion bodies for bio-based products: curse or blessing?, Appl. Microbiol. Biotechnology. 103 (2019) 1143–1153, https://doi.org/10.1007/s00253-018-9569-1.

[20] U. Krauss, V.D. Jäger, M. Diener, M. Pohl, K.E. Jaeger, Catalytically-active inclusion bodies—Carrier-free protein immobilizates for application in biotechnology and biomedicine, J. Biotechnol. 258 (2017) 136–147, https://doi.org/10.1016/j.jbiotec.2017.04.033.

[21] P. Singhvi, A. Saneja, S. Srichandan, A. K. Panda, Bacterial inclusion bodies: A treasure trove of bioactive proteins, Trends Biotechnol. 38 (2020) 474–486, https://doi.org/10.1016/j.tibtech.2019.12.011.

[22] I. Martín-Arjol, J.L. Llacuna, A. Manresa, Yield and kinetic constants estimation in the production of hydroxy fatty acids from oleic acid in a bioreactor by *Pseudomonas aeruginosa* 42A2, Appl. Microbiol. Biotechnol, 98 (2014) 9609–9621, https://doi.org/10.1007/s00253-014-5996-9.

[23] J. Sambrook, E.F. Fritsch, T. Maniatis Molecular cloning: a laboratory manual. Second edition, Cold Spring Harbor Laboratory Press, New York, 1998.

[24] M.M. Bradford, A rapid and simple method for the quantitation of micrograms quantities of protein utilizing the principle of protein-dye binding, Anal. Biochem. 72 (1976) 248–254, https://doi.org/10.1006/abio.1976.9999.

[25] U.K. Laemmli, Cleavage of structural protein during the assembly of the head of bacteriophage T4, Nature 227 (1970) 660-685, https://doi.org/10.1038/227680A0.

[26] E. Rodríguez-Carmona, O. Cano-Garrido, J. Seras-Franzoso, A. Villaverde, E. García-Fruitós, Isolation of cell-free bacterial inclusion bodies, Microb. Cell Fact. 9 (2010) 71, https://doi.org/10.1186/1475-2859-9-71.

[27] O. Cano-Garrido, A. Sánchez-Chardi, S. Parés, I. Giró, W.I. Tatkiewicz, N. Ferrer-Miralles, I. Ratera, A. Natalello, R. Cubarsi, J. Veciana, À. Bach, A. Villaverde, A. Arís, E. Garcia-Fruitós, Functional protein-based nanomaterial produced in microorganisms recognized as

safe: A new platform for biotechnology, Acta Biomater. 43 (2016) 230–239, https://doi.org/10.1016/j.actbio.2016.07.038.

[28] M. Carrió, N. González-Montalbán, A. Vera, A. Villaverde, S. Ventura, Amyloid-like properties of bacterial inclusion bodies, J. Mol. Biol. 347 (2005) 1025–1037, https://doi.org/10.1016/j.jmb.2005.02.030.

[29] F.S. Altschul, T.L. Madden, A.A. Schaffer, J. Zhang, Z. Zhang, W. Miller, D.J. Lipman, Gapped BLAST and PSI-BLAST: a new generation of protein database search programs, Nucleic Acids Res. 25 (1997) 3389–3402, https://doi.org/10.1093/nar/25.17.3389.

[30] D. Ami, A. Natallelo, P. Gatti-Lafranconi, M. Lotti, S. Doglia, Kinetics of inclusion body formation studied in intact cells by FT_IR spectroscopy, Febs Let. 679 (2005) 3433–3436, https://doi.org/10.1016/j.febslet.2005.04.085.

[31] K.R. Kim, D.K.K. Oh, J, Kim, Production of hydroxy fatty acids by microbial fatty acid-hydroxylation enzymes, Biotechnol. Adv. 31 (2013) 1473–85, https://doi.org/10.1016/j.biotechadv.2013.07.004.

[32] W.S. Bowers, H. Hoch, P. Evans, M. Katayama, Thallophytic allelopathy: Isolation and identification of laetisaric acid, Science 232 (1986) 105–106, https://doi.org/10.1126/science.232.4746.105

[33] I.D. Brodowsky, E.H. Oliw, Biosynthesis of 8R-hydroperoxylinoleic acid by the fungus *Laetisaria arvalis*, Biochim. Biophys. Acta 1168 (1993), 68–72, https://doi.org/10.1016/0005-2760(93)90267-d.

[34] I.D. Brodowsky, M. Hamberg, E.H. Oliw, A linoleic acid (8R)-dioxygenase and hydroperoxide isomerase of the fungus *Gaeumannomyces graminis*. Biosynthesis of (8R)-hydroxylinoleic acid and (7S,8S)-dihydroxylinoleic acid from (8R)-hydroperoxylinoleic acid, J. Biol. Chem. 267 (1992) 14738–45, http://www.ncbi.nlm.nih.gov/pubmed/1634517.

[35] C. Su, E.H. Oliw, Purification and characterization of linoleate 8-dioxigenase from the fungus *Gaeumannomyces graminis* as a novel hemoprotein, J. Biol. Chem. 271 (1996) 14112–14118, https://doi.org/10.1074/jbc.271.24.14112.

[36] U. Garsha, F. Jernerén, D.W. Chung, N. Keller, M. Hamberg, E.H. Oliw, Identification of dioxygenases required for *Aspergillus* development, J Biol Chem. 282 (2007) 34707–34718, https://doi.org/10.1074/jbc.M705366200.

[37] I. Lang, A. Göbel, I. Heilmann, I. Freussner, A lipoxygenase with linoleate diol synthase activity in *Nostoc* sp. PCC 7120, Biochem. J. 410 (2008) 347–357. https://doi.org/10.1042/BJ20071277.

[38] E. García-Fruitós, M. González-Montalban, N. Morell, A. Vera, R.M. Ferraz, A. Arís, S. Ventura, A. Villaverde, Aggregation as bacterial inclusion bodies does not imply inactivation of enzymes and fluorescent proteins, Microb. Cell Fact. 4 (2005) 27–32, https://doi.org/10.1186/1475-2859-4-27.

[39] Š. Peternel, R. Komel, Active protein aggregates produced in *Escherichia coli*, Int. J. Mol. Sci. 12 (2011) 8275–8287, https://doi.org/10.3390/ijms12118275.

[40] T. Vazhnova, D.B. Lukyanov, Fourier self-deconvolution of the IR spectra as a tool for investigation of distinct functional groups in porous materials: Brønsted acid sites in zeolites, Anal. Chem. 85 (2013) 11291–11296, https://doi.org/10.1021/ac4020337.

[41] M. Morell, R. Bravo, A. Espargaró, F.X. Avilés, X. Fernàndez-Busquets, S. Ventura, Inclusion bodies: Specificity in their aggregation process and amyloid-like structure, Biochim. Biophys. Acta - Mol. Cell Res. 1783 (2008) 1815–1825, https://doi.org/10.1016/j.bbamcr.2008.06.007.

[42] M.R. Nilsson, Techniques to study amyloid fibril formation, Methods. 34 (2004) 151–160, https://doi.org/10.1016/j.ymeth.2004.03.012.

[43] N.S. de Groot, R. Sabate, S. Ventura, Amyloids in bacterial inclusion bodies, Trends Biochem. Sci. 34 (2009) 408–416, https://doi.org/10.1016/j.tibs.2009.03.009.

[44] A. Villaverde, J.L. Corchero, J. Seras-Franzoso, E. García-Fruitós, Functional protein aggregates: just the tip of the iceberg, Nanomedicine. 10 (2015) 2881–2891, https://doi.org/10.2217/nnm.15.125.

[45] N.S. de Groot, S. Ventura, Effect of temperature on protein quality in bacterial inclusion bodies, FEBS Lett. 580 (2006) 6471–6476, https://doi.org/10.1016/j.febslet.2006.10.071.

[46] S. Shoja Chaghervand, Characterization of the Enzymes Involved in the Diolsynthase Pathway in *Pseudomonas aeruginosa*, PhD Thesis, University of Barcelona, 2019, https://tdx.cat/browse?value=Shoja+Chaghervand%2C+Shirin&type=author.

[47] U. Rinas, E. Garcia-Fruitós, J.L. Corchero, E. Vázquez, J. Seras-Franzoso, A. Villaverde, Bacterial inclusion bodies: discovering their better half, Trends Biochem. Sci. 42 (2017) 726–737, https://doi.org/10.1016/j.tibs.2017.01.005.

[48] M. Lynch, V. Katju, The altered evolutionary trajectories of gene diuplicates, Trends Genet. 20 (2004) 544–549, https://doi.org/10.1016/j.tig.2004.09.001.

[49] R.A. Brash, N.P. Niraula, W.E. Boeglin, Z. Mashhadi, An ancient relative of cyclooxygenase in cyanobacteria is a linoleate 10S-dioxygenase that works in tandem with a catalase-relate protein with specific 10S hydroperoxide liase activity, J. Biol. Chem. 289 (2014) 13101–13111, https://doi.org/10.1074/jbc.M114.55590455904.

Tables

Table I. Plasmids and strain used in this work.

Table II. Products detected in the supernatant due to the transformation of oleic acid by selected proteobacteria. H(P)OME: 10*S* hidroperoxid-8*E*-octadecenooic acid; HOME: 10*S*-hydroxy-8*E*-octadecenoic acid; DiHOME: 7,10dihydroxy-8*E*-ocatadecenoic acid.

Figure Legend

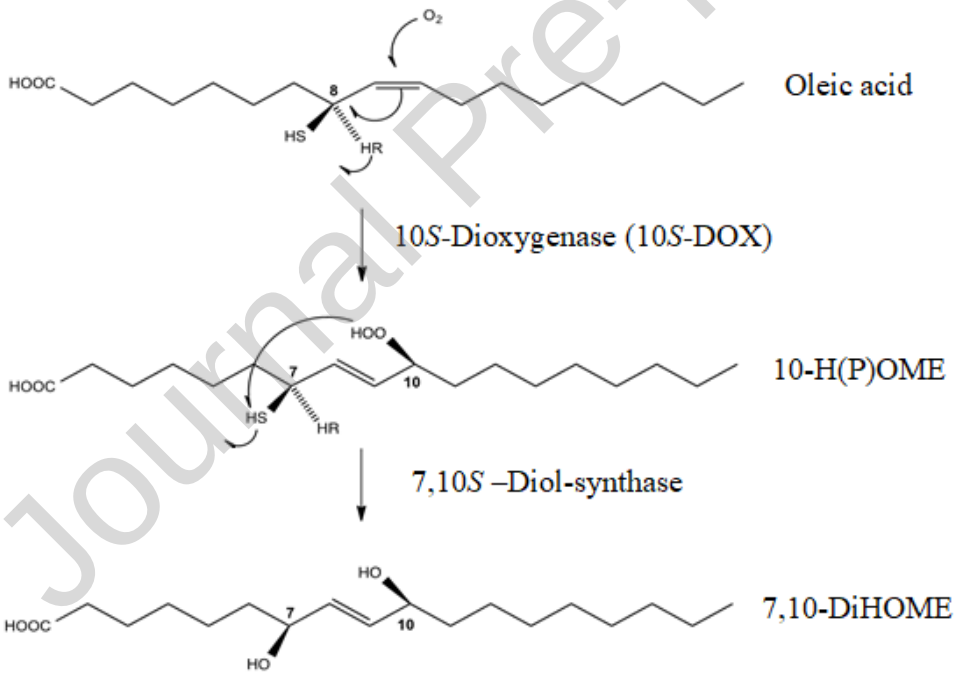

Fig. 1. Synthesis of (10*S*) hydro(per)oxy-(8*E*)8 octadecenoic acid (10-H(P)HOME) and 7*S*,10*S*)-dihydroxy-(8*E*)-octadecenoic acid (7,10-DiHOME) from oleic acid by *P. aerugi*nosa,

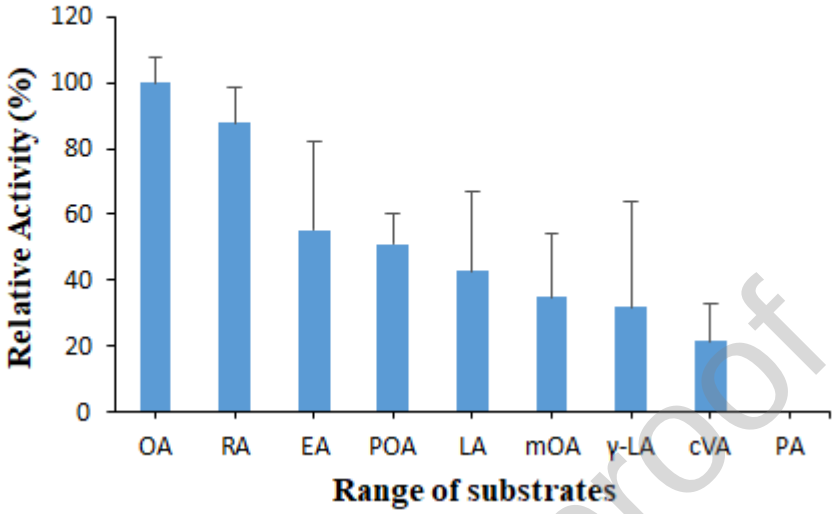

Fig. 2. Substrate specificity of 10*S*-DOX. The rate of biotransformation of each substrate is expressed relative to the rate of OA transformation (100%); RA: ricinoleic acid; EA: elaidic acid; POA: palmitoleic acid; LA: linoleic acid; mOA: methyl-(9*Z*)-octadecenoate acid; γ-LA: gamma-linolenic acid; cVA: cis-vaccenic acid; PA: petroselinic acid. Activities were determined as described in Material and methods using *E. coli* DH5α/pMMB as a control (see Table 1 of M & M section).

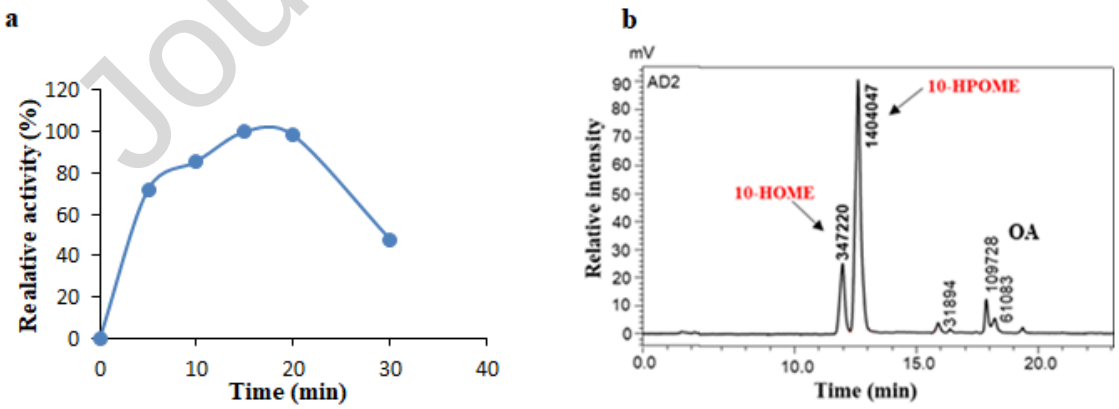

Figure 3. (a) Time course of the production of 10*S*-H(P)OME with *P. putida* (pBBR-77) plot giving % of relative production of H(P)OME with *P. putida* (pBBR-77). (b) RP-HPLC of H(P)OME was produced under standard conditions (20 min at 30 ºC and 150 rpm).

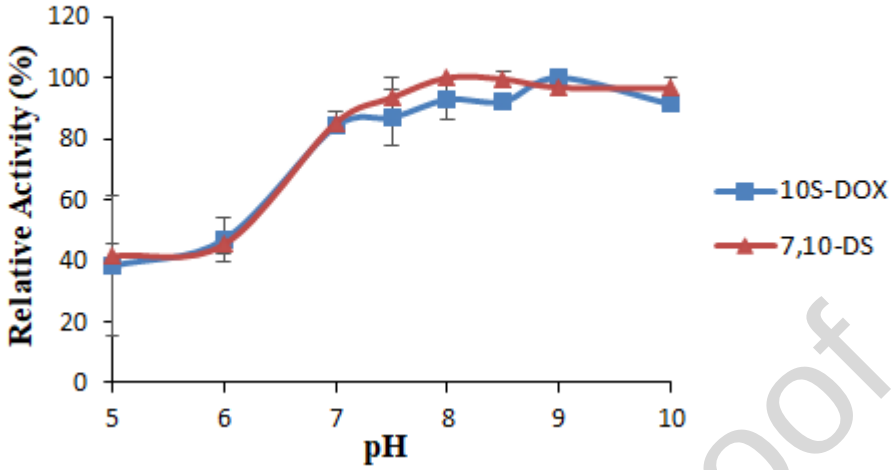

Fig. 4. Effect of different pH values of the reaction on 10*S*-DOX and 7,10-DS activity in 20mM Britton-Robinson buffer at 30 ºC and pH ranging from 5.0 to 10. Samples were incubated for 15 min at 30 ºC.

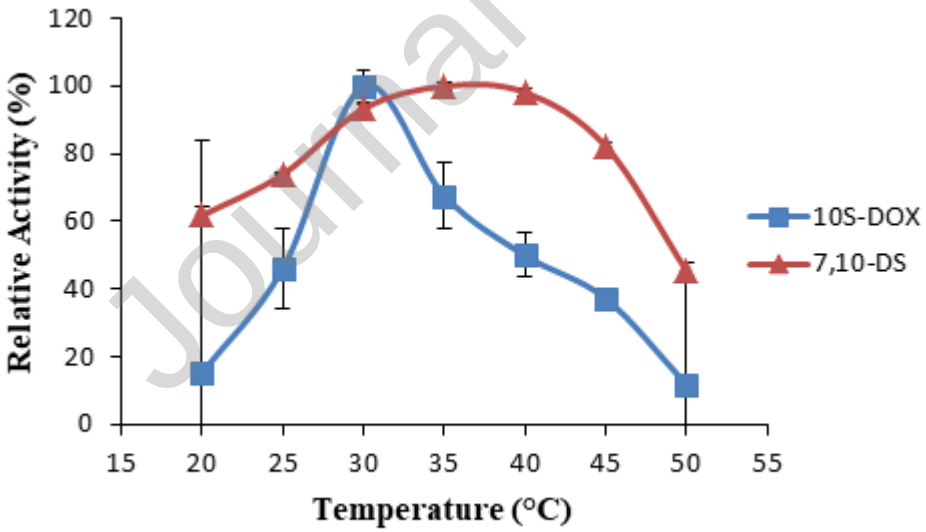

Fig. 5. Effect of different reaction temperatures from 20 to 70 ºC on 10*S*-DOX and 7,10-DS activity. Samples were incubated for 15 min at the corresponding temperature.

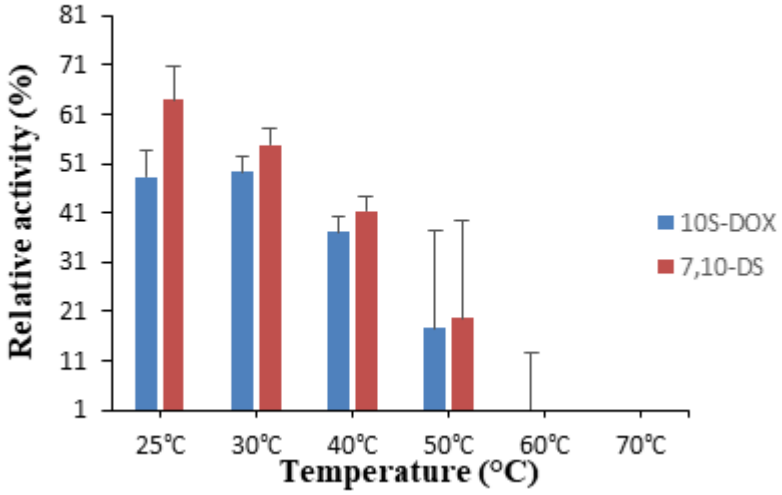

Fig. 6. Thermal stability was analyzed by incubating the enzymes (10*S*-DOX and 7,10-DS) at 25-60 °C for 15 min at 30 ºC in 50 mM Tris-HCl buffer pH 7.0. The control refers to non-treated cell extract was measured at 30 °C and represents 100% of enzymatic activity.

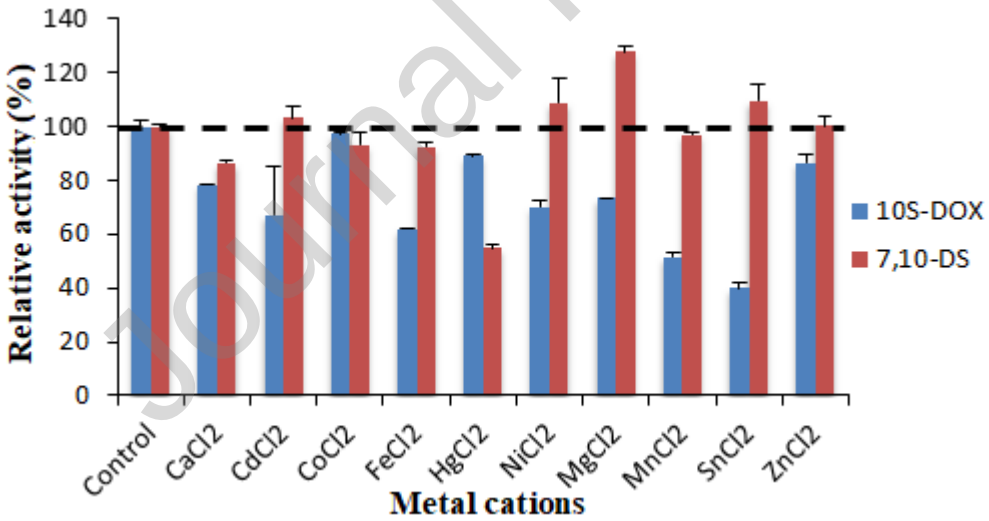

Fig. 7. Effect of cations on the activity of 7,10-DS and 10*S*-DOX enzymes. The control was incubated at optimal conditions with no cation addition and is referred to like 100% of enzymatic activity. Samples were incubated for 15 min at 30 ºC.

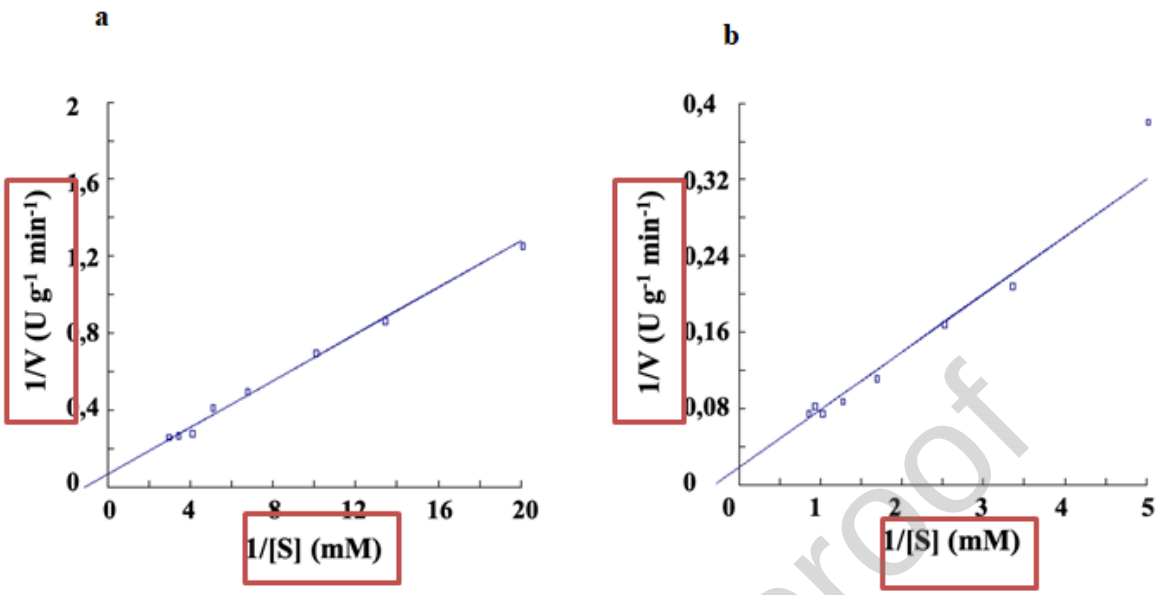

Fig. 8. (a) Lineweaver-Burk plot for Km and Vmax values of the 10*S*-DOX enzyme 15 min at 30 ºC. Assay condition was pH 7.0 in the presence of different concentrations of OA (0.05-0.35 mM). (b) Lineweaver-Burk plot for Km and Vmax values of the 7,10-DS enzyme 15 min at 30 ºC. Assay condition was pH 7.0 in the presence of different concentrations of 10-H(P)OME (0.2-1.2 mM).

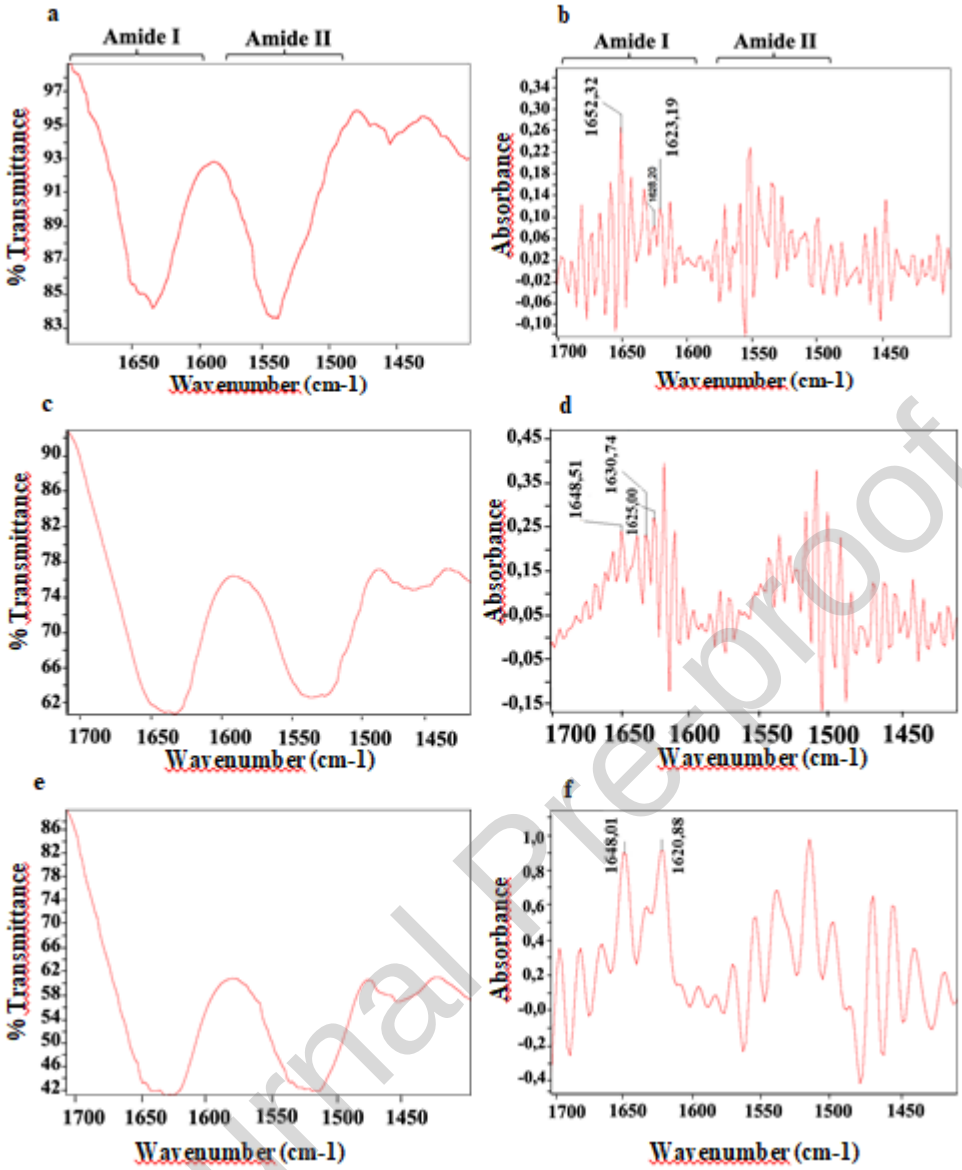

Figure 9. FT-IR: a) Row spectra of soluble protein, (b) deconvoluted spectra of soluble protein: α-helix (1652), β-sheets (1623 and 1628) and (c) row spectra of purified IBs-77, (d) deconvoluted spectra of purified IBs-77: α-helix (1648), β-sheets (1625 and 1630). (e) row spectra of purified IBs-78, (f) deconvoluted spectra of purified IBs-78: α-helix (1648), β-sheets (1620).

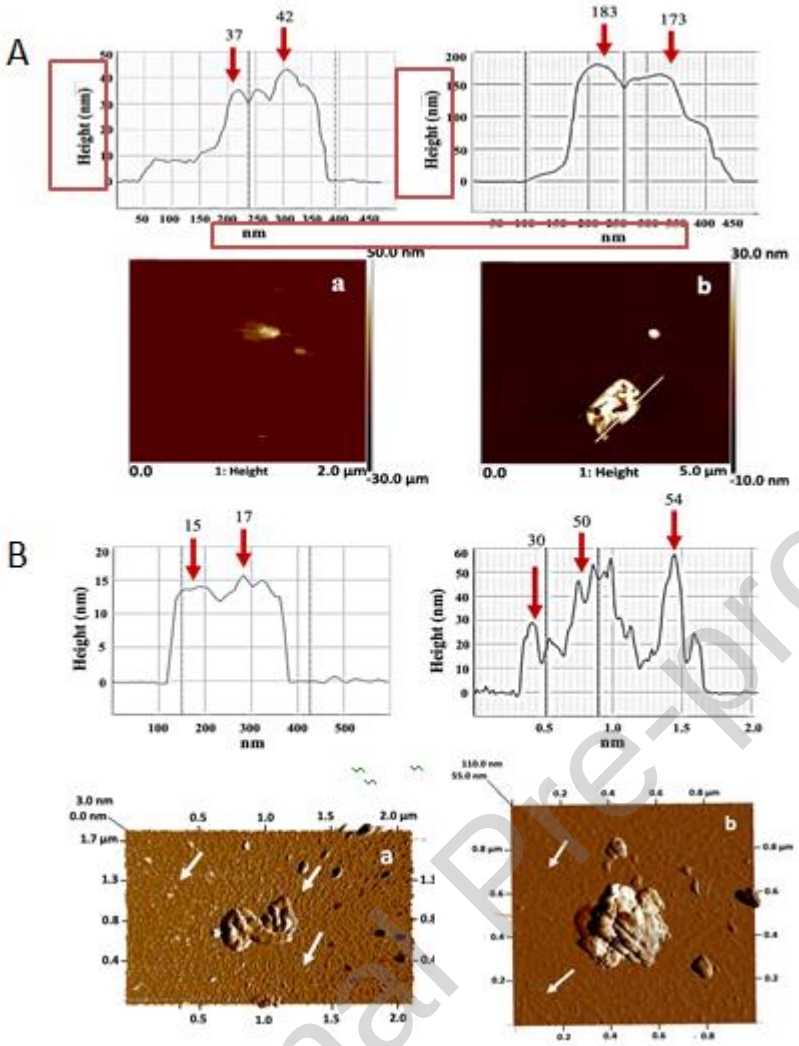

Figure 10. a) Amplitude AFM images of Individual IBs-77 after 30 min PK digestion. (b) IBs-78 after 30 min PK treatment. The diagram represents the profile drawn by the cantilever. Arrows indicates the profile defined by the cantilever. Height was measured in nm.

TABLES

Table 1. Plasmids and strains used in this work.

Strains	Relevant characteristics	Reference
E. coli DH5α	supE44ΔlacU169 (ϕ80lacZΔM15) hsR1 RecA1 endA1 gyrA96thi-1relA1	Invitrogen
E. coli DH5α/pMMB-77	CmR, carrying *PA2077* gene (10-*dox*)	[13]
E. coli DH5α/pMMB-78	CmR, carrying *PA2078* gene (7,10-*ds*)	[13]
P. putida KT2440	Wild type, GRAS (Generally Recognize as Safe) strain	[13]
P. putida KT2440/pBB-77	CmR, carrying pBBR-77 (10-*dox*)	[14]
P. aeruginosaPAO1(ΔDS)/pBB-77	CmR, ΔPA2078 mutant carrying pBBR-77 (10-*dox*)	[13]

Table II. Products detected in the supernatant due to the transformation of oleic acid by selected proteobacteria. H(P)OME: (10*S*)-hydro(per)oxy-(8*E*)-octadecenoic acid; DiHOME: (7*S*,10*S*)-dihydroxy-(8*E*)-ocatadecenoic acid.

Strains	**H(P)OME**	**DiHOME**
Aeromonas allosaccharophila	–	+
Aeromonas caviae	+	+
Aeromonas bivalvium	+	+
Aeromonas hydrophila	–	+
Aeromonas salmonicida	+	+
Pseudoalteromonas atlantica	+	+
Pseudoalteromonas aliena	–	+
Pseudoalteromonas antarctica	+	+
Shewanella woodyi	+	+
Shewanella putrefaciens	–	–
Shewanella vesiculosa	+	–
Shewanella hanedai	+	+
Pseudomonas lini	+	+
Pseudomonas tolassi	+	+
Pseudomonas taetrolens	–	+
Pseudomonas fluorescens	+	+
Pseudomonas fragi	–	+
Pseudomonas lundensis	–	–
Pseudomonas oleovorans	–	–
Pseudomonas psychrophyla	–	–
Pseudomonas putida	–	–
Thauera aminoaromatica	+	–
Ensifer fredii	+	+

Conflict of interest

Author 1 declare she has not conflict of interest. Author 2 declare she has not conflict of interest. Author 3 declare she has not conflict of interest. Author 4 declare she has not conflict of interest. Author 5 declare she has not conflict of interest

Ethical statement

this article does not contain any studies with human participants or animals performed by any of the authors

Informed consent

informed contains was obtained from all of individual participants included in the study

Graphical abstract

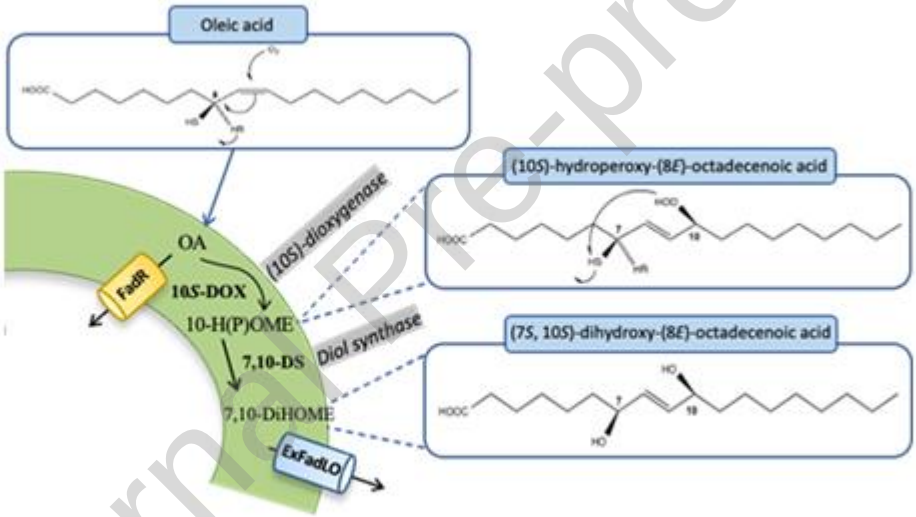

Highlights

- Biochemical characterization of recombinant 10*S*-dioxygenase (10*S*-DOX) and 7,10-diolsynthase (7,10-DS) from *P. aeruginosa.*
- Production of 10*S*-hydroxy(per)-oxi-(8*E*)-octadecenoic acid using recombinant 10*S*-DOX.
- Aggregate proteins 10*S*-DOX and 7,10-DS were characterized as inclusion bodies.
- Oleic acid conversion by diol syntase system is not restricted to *P. aeruginosa*